THE JOURNAL OF PHYSICAL CHEMISTRY Letters

Letter

pubs.acs.org/JPCL

Atomic-Scale Perspective of Ultrafast Charge Transfer at a Dye–Semiconductor Interface

Katrin R. Siefermann,[†,□] Chaitanya D. Pemmaraju,[‡] Stefan Neppl,[†] Andrey Shavorskiy,[§] Amy A. Cordones,[∥,●] Josh Vura-Weis,[∥,△] Daniel S. Slaughter,[†] Felix P. Sturm,[†] Fabian Weise,[†,▲] Hendrik Bluhm,[§] Matthew L. Strader,[§,▼] Hana Cho,[§] Ming-Fu Lin,[†,∥,△] Camila Bacellar,[†,∥] Champak Khurmi,[†,%] Jinghua Guo,[#] Giacomo Coslovich,[⊥] Joseph S. Robinson,[⊥,▽] Robert A. Kaindl,[⊥] Robert W. Schoenlein,[†,⊥] Ali Belkacem,[†] Daniel M. Neumark,[†,¶] Stephen R. Leone,[†,∥,○] Dennis Nordlund,[◆] Hirohito Ogasawara,[◆] Oleg Krupin,[▽,¶] Joshua J. Turner,[▽] William F. Schlotter,[▽] Michael R. Holmes,[▽] Marc Messerschmidt,[▽,&] Michael P. Minitti,[▽] Sheraz Gul,[#,+] Jin Z. Zhang,[+] Nils Huse,[■] David Prendergast,[‡] and Oliver Gessner*[,†]

[†]Ultrafast X-ray Science Laboratory, Chemical Sciences Division, Lawrence Berkeley National Laboratory, Berkeley, California 94720, United States

[‡]The Molecular Foundry, Lawrence Berkeley National Laboratory, Berkeley, California 94720, United States

[§]Chemical Sciences Division, Lawrence Berkeley National Laboratory, Berkeley, California 94720, United States

[∥]Department of Chemistry, University of California, Berkeley, California 94720, United States

[⊥]Materials Sciences Division, Lawrence Berkeley National Laboratory, Berkeley, California 94720, United States

[#]Advanced Light Source, Lawrence Berkeley National Laboratory, Berkeley, California 94720, United States

[▽]Linac Coherent Light Source, SLAC National Accelerator Laboratory, Menlo Park, California 94025, United States

[○]Department of Physics, University of California, Berkeley, California 94720, United States

[◆]SLAC National Accelerator Laboratory, Menlo Park, California 94025, United States

[¶]European XFEL GmbH, 22761 Hamburg, Germany

[+]Department of Chemistry and Biochemistry, University of California, Santa Cruz, California 95064, United States

[■]Physics Department, University of Hamburg and Max-Planck Institute for Structure and Dynamics of Matter, 22761 Hamburg, Germany

Supporting Information

ABSTRACT: Understanding interfacial charge-transfer processes on the atomic level is crucial to support the rational design of energy-challenge relevant systems such as solar cells, batteries, and photocatalysts. A femtosecond time-resolved core-level photoelectron spectroscopy study is performed that probes the electronic structure of the interface between ruthenium-based N3 dye molecules and ZnO nanocrystals within the first picosecond after photoexcitation and from the unique perspective of the Ru reporter atom at the center of the dye. A transient chemical shift of the Ru 3d inner-shell photolines by (2.3 ± 0.2) eV to higher binding energies is observed 500 fs after photoexcitation of the dye. The experimental results are interpreted with the aid of ab initio calculations using constrained density functional theory. Strong indications for the formation of an interfacial charge-transfer state are presented, providing direct insight into a transient electronic configuration that may limit the efficiency of photoinduced free charge-carrier generation.

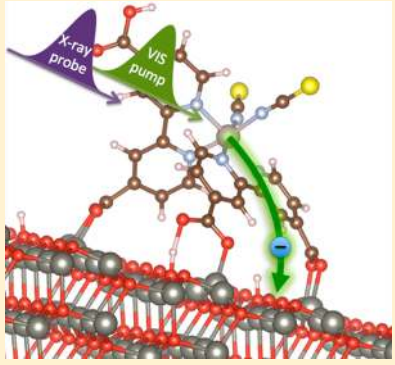

SECTION: Spectroscopy, Photochemistry, and Excited States

Interfacial charge-transfer dynamics play a crucial role in a number of emerging photoelectrochemical technologies, in particular, for photovoltaic and photocatalytic applications. An atomic level understanding of the transient electronic configurations that govern the conversion efficiencies of photoinduced excitations into separate charges is essential in order to exploit the full potential of novel photon-harvesting schemes. Dye-sensitized solar cells (DSSCs) are a particularly prominent example of chemically engineered photovoltaic devices that convert sunlight into electricity through the combination of an efficient light absorber

Received: June 20, 2014
Accepted: July 25, 2014
Published: July 25, 2014

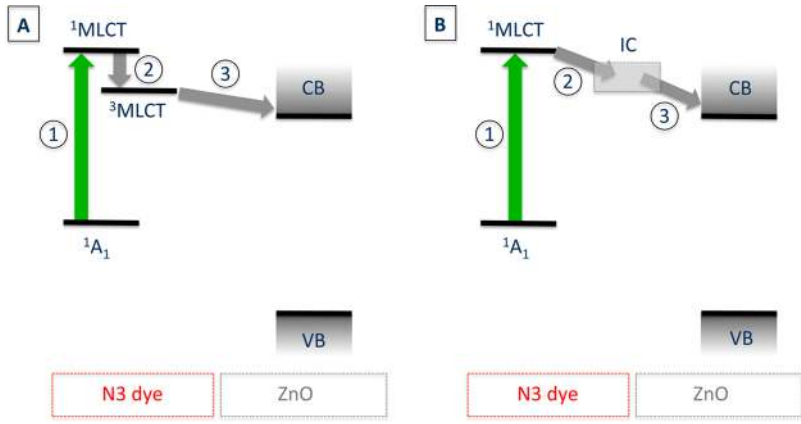

Figure 1. Two competing models for the sequence of charge-injection at N3 dye−ZnO nanocrystal interfaces after photoexcitation (step 1) of the dye. (A) Two-state injection model in which the electron is temporarily retained in a ^{3}MLCT state (step 2) on the dye molecule. (B) Intermediate interfacial state model in which the electron is temporarily retained in an interfacial complex (IC, step 2) at the dye−semiconductor interface. In both cases, step 3 indicates the release of the electron into the ZnO conduction band (CB) as a free charge carrier.

(dye molecules) with a nanostructured semiconductor substrate.[1−4] Dye−semiconductor charge injection mechanisms have been investigated in numerous studies with a particular emphasis on the associated injection rates.[5−22] However, owing to the complexity of the interfacial configurations, an unambiguous interpretation of the experimental findings is often challenging, in particular, on a level of detail commensurate with advanced theoretical predictions.[3,23−26] Here a femtosecond time-resolved X-ray photoelectron spectroscopy (TRXPS[27,28]) study is presented that probes the transient interfacial electronic configuration of the ruthenium-based dye N3 (bis(isothiocyanato)bis(2,2′-bipyridyl-4,4′-dicarboxylato)-ruthenium(II)) attached to a zinc oxide (ZnO) nanoparticle film within the first picosecond after photoexcitation of the dye. The atomic-site-specific TRXPS results in combination with density functional theory (DFT) calculations provide strong indications for a transient charge-transfer state that is established across the N3−ZnO interface within 500 fs. The findings are of direct relevance with respect to a decade-long controversy surrounding the fundamental electronic dynamics that underlie performance differences in TiO_2- and ZnO-based DSSCs.

A number of studies have demonstrated that the differences between these systems, for example, in the critical photon-to-current conversion efficiencies cannot be explained by common system benchmarks such as the dye−semiconductor energy level alignment or the electron mobility of the substrate material.[13,29,30] Instead, the atomic-scale electronic coupling and transient interfacial electronic structure are believed to play key roles in determining the device function.[9−13,31] Ultrafast time-domain studies in the optical, infrared, and terahertz regimes have identified distinct differences between the dynamic response of dye−ZnO and dye−TiO_2 interfaces.[5,8−13,17] In particular, transient signals from ZnO-based dye-sensitized systems are marked by prominent "slow" components, which evolve on time scales ranging from a few to hundreds of picoseconds. These response times are orders of magnitude longer than the typical sub-50 fs dynamics of TiO_2-based interfaces and are, therefore, often associated with ZnO cell performance limitations.[5,8−13] While these dramatic differences of time scales are consistently detected in a variety of experiments, their physical origin has long been a matter of debate, leading to two competing models for the underlying mechanisms (Figure 1).

In the two-state injection model[5−7] (Figure 1A), only a small fraction of the initially excited singlet metal-to-ligand charge-transfer (^{1}MLCT) states directly injects an electron into the conduction band (CB) of ZnO within <100 fs. The majority of dye molecules undergo intramolecular relaxation to the metastable ^{3}MLCT state owing to reduced electronic coupling between the dye and the semiconductor and a low density of charge accepting states in the substrate. Subsequent electron injection from the ^{3}MLCT state is suggested to take place on ∼100 ps time scales; that is, the electrons are temporarily retained on the molecular dye.[5] In the intermediate interfacial state model[8−13] (Figure 1B), photoexcitation of the dye leads to fast (≤100 fs to ≤5 ps)[8,10] formation of an interfacial complex (IC) at the dye−semiconductor interface with either neutral exciplex or ionic charge-transfer character.

Time-domain experiments suggest that the decay time scales of such an IC to release a mobile electron into the semiconductor substrate may range from ∼2 to ∼150 ps.[8,10−13] Thus, in the intermediate interfacial state model, the electrons are temporarily retained at the interface between the dye and the substrate. While it is generally accepted that the increased retention time of the electrons either on the dye (Figure 1A) or at the dye−semiconductor interface (Figure 1B) will reduce the overall efficiency for free charge-carrier generation and therefore the device performance of ZnO-based photoelectrochemical devices, a clear identification of one of the mechanisms as the predominant electronic bottleneck has been hampered by the lack of a unique spectroscopic signature for either model.

The combination of femtosecond time-resolved inner-shell photoelectron spectroscopy with a detailed theoretical modeling presented here strongly supports the existence of a transient intermediate state located at the interface between the ZnO substrate and the N3 dye, which is populated within 500 fs after photoexcitation and has a lifetime well beyond 1 ps. The identification of the intermediate state character becomes possible through the unique capability of novel femtosecond X-ray spectroscopy techniques to monitor ultrafast local valence electron dynamics from the perspective of distinct atomic sites. Here the Ru metal center of the dye is chosen as a reporter atom during the interfacial charge-transfer process. In the experiment, N3-molecules adsorbed to a film of ZnO nanocrystals are excited by a 50 fs optical (535 nm) pump pulse. Interfacial charge-transfer dynamics are monitored by transient changes in femtosecond time-resolved XPS spectra. The measurements are performed at the Soft X-ray Materials Science (SXR) instrument of the Linac Coherent Light Source (LCLS) using <100 fs long

dx.doi.org/10.1021/jz501264x | J. Phys. Chem. Lett. 2014, 5, 2753−2759

X-ray pulses at a photon energy of 850 eV. (See Supporting Information S2 for details.)

Femtosecond Time-Resolved X-ray Photoelectron Spectra. Figure 2A shows two photoelectron spectra in the binding energy range between E_b = 276 and 293 eV recorded with (red, solid) and without (blue, dashed) the optical pump pulse preceding the X-ray pulse by 500 fs. The photoelectron spectra are marked by three prominent peaks corresponding to the Ru $3d_{5/2}$ line (E_b = 280.6 eV) and two C 1s lines associated with carbon atoms in the pyridine rings (E_b = 284.8 eV) and the carboxyl groups (E_b = 288.3 eV) of the dye.[32]

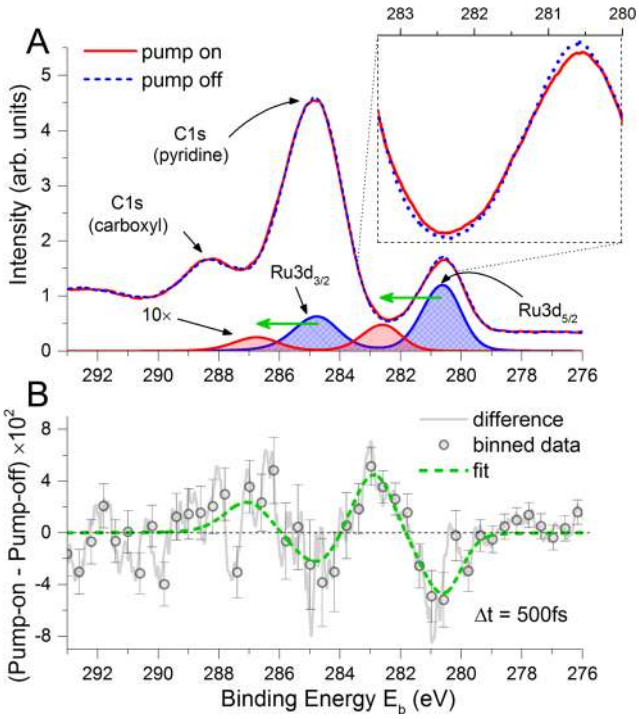

Figure 2. (A) Photoelectron spectra of N3/ZnO in the region of the C 1s and Ru 3d photolines recorded with (red, solid) and without (blue, dashed) the optical pump pulse preceding the X-ray probe pulse by 500 fs. The filled curves represent the Ru $3d_{3/2,5/2}$ doublet before (blue, cross-hatched) and after (red) photoexcitation of the dye. (B) Difference between pump-on and pump-off spectra at a pump−probe time delay of 500 fs (gray line). Circles correspond to the difference spectrum, rebinned to match the energy resolution of the experiment. Error bars indicate ±1 standard deviation uncertainty ranges. The dashed green fit curve is based on a model that describes the entire spectral change by a transient chemical shift of the Ru 3d signal as indicated by the green arrows in panel A.

The Ru $3d_{3/2}$ line (E_b = 284.8 eV) and the C 1s line from the thiocyanate groups (E_b = 286.0 eV, not shown) are covered by the much more intense pyridine C 1s peak.[32] The inset (top, right) shows an enlarged section of the spectrum in the region of the Ru $3d_{5/2}$ line. The pump−pulse induces a decrease in the ground state Ru $3d_{5/2}$ signal (blue, dashed) and a complementary increase in signal at ∼2 eV higher binding energies between the Ru $3d_{5/2}$ peak and the shoulder of the pyridine C 1s peak.

The pump−pulse-induced spectral change can be seen in more detail in Figure 2B, which shows the difference between the pump-on and pump-off spectra. The difference signal exhibits a local minimum at the position of the Ru $3d_{5/2}$ peak and a local maximum at a ∼2 eV higher binding energy, replicating the trend from Figure 2A. A second minimum is located at the position of the Ru $3d_{3/2}$ peak and a second maximum at ∼2 eV higher binding energies. This observation indicates that 500 fs after photoexcitation the fraction of molecules excited by the optical pump−pulse experiences an increase in effective binding energy E_b of both Ru 3d spin−orbit components on the order of ∼2 eV.

The dashed green line in Figure 2B is the result of a fit based on the assumption that the excitation-induced difference between the pump-on and pump-off spectra can be described entirely by a transient chemical shift of the Ru 3d features. This results in a fit procedure with only two free parameters, the fraction F of the Ru 3d signal that exhibits the transient shift and the magnitude ΔE_b of the shift. An accurate description of the Ru $3d_{3/2,5/2}$ doublet (Figure 2A, blue and red filled curves) is derived from synchrotron measurements on a Ru(0001) crystal taking into account the natural line shapes and the instrumental response functions of the synchrotron- and the LCLS-based XPS spectrometers. (See S4.1 in the Supporting Information for details.) The good agreement of the fit with the data as illustrated in Figure 2B supports the ad-hoc imposed description of the difference signal by the transient shift of the Ru doublet, while other signals, such as the four times more intense C 1s signal from the pyridine group, contribute to a much smaller amount. A quantitative analysis of the absolute fit reliability is described in the SI (S4.2).

Least-square fits are performed for two data sets at pump−probe time delays of Δt = 500 fs and Δt = 1 ps (S4 in the Supporting Information). The central experimental findings of this study are (a) the Ru 3d doublet exhibits a transient chemical shift ΔE_b = (2.3 ± 0.2) eV to higher binding energies 500 fs after photoexcitation of the dye, (b) the doublet exhibits a very similar chemical shift ΔE_b = (1.9 ± 0.3) eV at 1 ps pump−probe delay, (c) possible photon-induced chemical shifts in the C 1s core

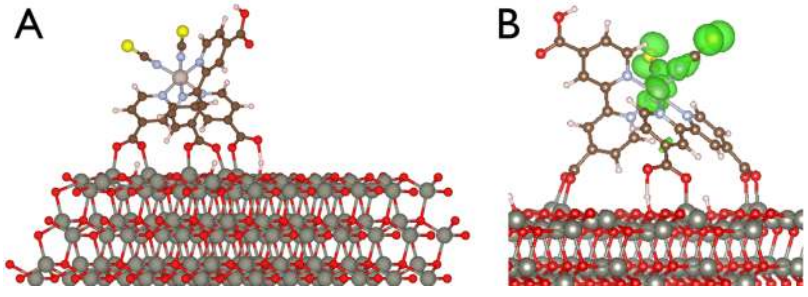

Figure 3. (A) Lowest energy adsorption geometry of N3 dye on wurtzite ZnO ($10\bar{1}0$). (B) HOMO orbital of N3 dye concentrated on the central Ru atom and the thiocyanate ligands. The iso-surfaces mark an electron density of 5% relative to the maximum value. Note the different viewing angles in panels A and B for improved clarity.

dx.doi.org/10.1021/jz501264x | *J. Phys. Chem. Lett.* 2014, 5, 2753−2759

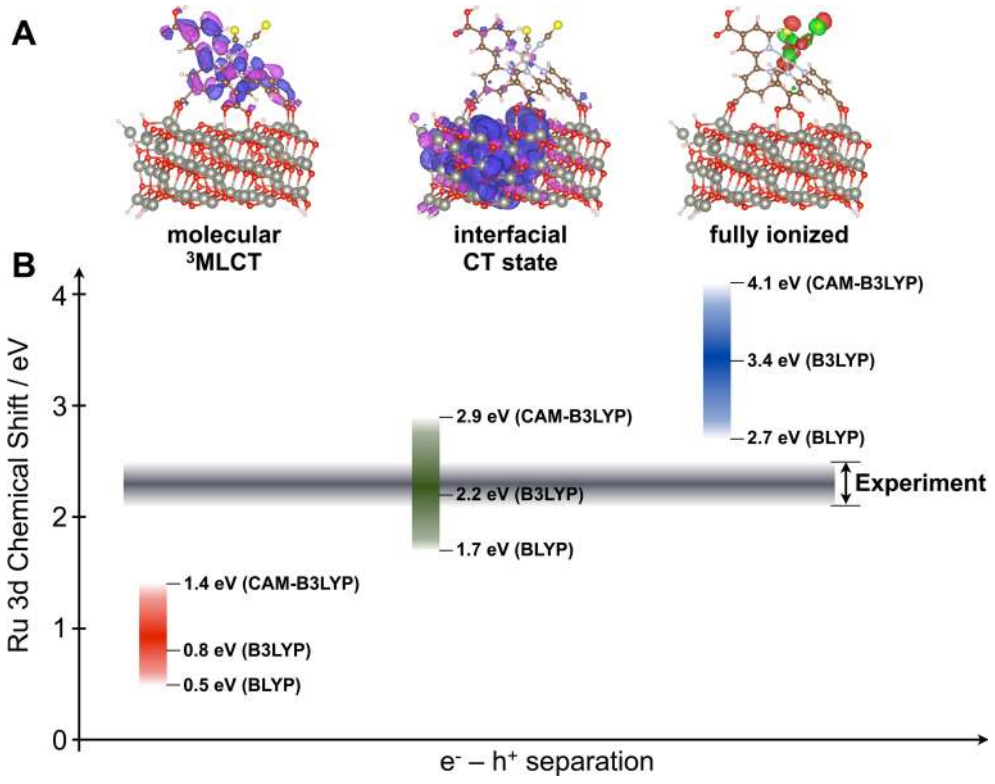

Figure 4. (A) Calculated electronic configurations for three limiting cases of transient electron–hole states (from left): molecular ^{3}MLCT state, interfacial CT state, and fully ionized state. For the ^{3}MLCT and CT states, the wave function of the excited electron is displayed, while for the fully ionized state the hole wave function is shown. (B) Calculated Ru 3d core level binding energy shifts obtained with three different functionals (BLYP, B3LYP, CAM-B3LYP). The gray band represents the experimentally determined shift of ΔE_b=(2.3 ± 0.2) eV at a delay of 500 fs after photoexcitation of the dye.

levels are much less pronounced and below our detection limit. The dye excitation fractions derived by the fit procedure are F = 4(±1)% and F = 7(±2)% for pump–probe delays of 500 fs and 1 ps, respectively.

Modeling of the Interface. The experimental results are interpreted with the aid of first-principles DFT calculations.[33,34] Figure 3A shows the lowest energy configuration of an N3 molecule adsorbed onto a wurtzite ZnO $(10\bar{1}0)$ surface modeled in a 2-D slab geometry. (See S5 in the Supporting Information for computational details.) In this configuration, the dye has three points of contact with the ZnO surface. Two of the four carboxyl groups are deprotonated and bound to the surface in a bidentate bridging mode. This picture is consistent with the results of a previous infrared spectroscopy study.[35] The detached protons passivate two nearby oxygen atoms of the ZnO surface. In addition, one carboxyl group coordinates via an O–Zn and an H–O interaction to the surface. This molecular conformation is found to be at least ∼1.3 eV more favorable in energy than any other adsorption geometry. Figure 3B shows the highest occupied molecular orbital (HOMO) of N3 attached to ZnO $(10\bar{1}0)$. The strong concentration of the HOMO on the central Ru atom and the thiocyanate ligands is consistent with previous experimental and theoretical studies.[18,19,23,24,32,36]

In an intuitive picture, the photoinduced removal of an electron from the HOMO of the dye molecule is expected to lead to a significant increase in inner-shell binding energies in those parts of the molecule where most of the HOMO electron density is localized. This is consistent with our experimental finding that the excitation-induced chemical shift is much more prominent in the Ru 3d doublet than in the C 1s carboxyl and pyridine signals. A transient chemical shift of the C 1s lines associated with the thiocyanate ligands cannot be ruled out, but it is challenging to detect its contribution to the overall signal due to the spectral overlap with the more intense carbon and ruthenium signals in the vicinity of ∼286 eV binding energy.[32]

The goal of the theoretical analysis is to identify a length-scale of charge separation between the optically excited electron and hole densities that is consistent with the observed transient core-level shift ΔE_b. Valence excited electronic configurations and associated ΔE_b are calculated employing a constrained density functional theory (CDFT)[37] formalism and a finite cluster model of the N3/ZnO interfacial structure described above (see S5 for details).

Three limiting cases of transient electronic configurations are shown in Figure 4A: an intramolecular ^{3}MLCT state, an interfacial CT state, and a fully ionized dye adsorbed on a neutral ZnO substrate. In the ^{3}MLCT state, the excited electron is mostly located on the bipyridine ligands, which is consistent with recent calculations for solvated N3 molecules.[18] In the fully ionized configuration, the hole density largely mimics the HOMO of the ground-state molecule (Figure 3B), while the electron is assumed to be completely removed from the system. The electronic charge distribution of the interfacial CT state is constrained to simulate a configuration in which the excited electron is transferred to the ZnO substrate but not yet further separated from the dye cation. This configuration represents a charge-separation length scale that is intermediate to the ^{3}MLCT and the fully ionized configurations. In contrast with the fully ionized state, the ^{3}MLCT and interfacial CT states represent electronic excited states that require an additional constraining

dx.doi.org/10.1021/jz501264x | J. Phys. Chem. Lett. 2014, 5, 2753–2759

potential to be modeled in a DFT framework. As outlined in the SI (S5.4), this is facilitated by the CDFT approach.

The central finding of the theoretical analysis is summarized in Figure 4B. For each of the limiting electronic configurations depicted in Figure 4A, the chemical shift of the Ru 3d lines compared with the neutral ground state is estimated using three different DFT functionals (BLYP,[38,39] B3LYP,[40,41] CAM-B3LYP[42]).

These functionals span a wide range in their description of electronic screening (see S5.3 in the Supporting Information), leading to correspondingly wide ranges of estimated chemical shifts as signified by vertical colored bands. All chemical shifts increase consistently in the order BLYP, B3LYP, and CAM-B3LYP, consistent with the decrease in electronic screening effects along this sequence of functionals. The vertical bands in Figure 4B can therefore be interpreted as conservative uncertainty ranges of the DFT calculations. The gray band indicates the measured chemical shift (including the experimental uncertainty range) of the Ru $3d_{3/2,5/2}$ doublet 500 fs after photoexcitation of the dye.

The comparison between theory and experiment strongly favors the interfacial charge-transfer complex as the predominant electronic configuration during the early stages of the electron injection process. The similarity of chemical shifts measured at both time delays, 500 fs and 1 ps, indicates that the interfacial CT state has a lifetime significantly beyond 1 ps. This is in agreement with previous experimental findings on the decay time scales for the intermediate IC, which range from ∼2 to ∼150 ps.[8,10−13] The gap between the experimental findings (gray) and the theoretical uncertainty range for the fully ionized dye configuration (blue) in Figure 4B confirms the common notion that the charge injection process in the N3-ZnO system is relatively slow; that is, it proceeds on, at least, picosecond time scales. This long-lived intermediate state very likely contributes to the weak performance of ZnO-based DSSCs compared with TiO_2-based systems, as it increases the relative yield of unwanted loss processes such as electron−hole recombination. In contrast, for N3-TiO_2 and similar TiO_2-based systems, the injected electron becomes available as a free charge carrier on a sub-50 femtosecond time scale.[14−16]

The electronic configurations shown in Figure 4A and, in particular, the CDFT-based description of the interfacial CT state are model systems that represent distinct limiting cases of average electron−hole separation length scales. Further studies are needed to refine the exact nature of the intermediate state and to identify its physical origin. The estimated chemical shifts, however, are fairly insensitive to these details and vary predominantly with the average electron−hole distance. This supports the conclusion that the rate-limiting step for photoinduced free charge carrier generation at the N3/ZnO interface is characterized by an electronic configuration in which the electron has separated from the dye molecule but is still residing in close proximity to the dye cation at the dye/semiconductor interface. We note that a recent picosecond time-resolved X-ray absorption study lent support to the existence of intermediate interfacial charge-transfer complexes in solvated dye-sensitized TiO_2 nanocrystals based on the detection of surface trap states.[22]

The combined experimental and theoretical study presented here highlights the potential of TRXPS to monitor transient interfacial electron configurations with femtosecond time resolution and on an atomic level of detail. The novel method complements existing techniques such as time-resolved X-ray absorption and provides, in particular, exquisite surface sensitivity to monitor interfacial charge dynamics on application-like electrode configurations. Because of the moderate peak-power requirements of XPS, the technique will take full advantage of next-generation free-electron lasers (FELs) such as LCLS-II and the European XFEL, which will operate at significantly higher pulse repetition rates compared with existing ultrafast X-ray light sources.

■ EXPERIMENTAL AND COMPUTATIONAL METHODS

Sample Preparation. ZnO nanoparticles were synthesized by adding 50 mmol tetramethylammonium hydroxide (25% solution in methanol from Sigma-Aldrich) to a suspension of 50 mmol zinc acetate dihydrate (Merck) in 100 mL of anhydrous ethanol (Sigma-Aldrich). Extra solvent was decanted and ZnO particles were washed with ethanol. Thin films were obtained by spin coating 0.20 mL of the ZnO suspension on a Si(100) substrate, followed by drying and sintering in air. After ozone/UV cleaning, the thin films were immersed in 0.2 mM solution of N3 Ru dye (Aldrich) in absolute ethanol for 24 h. The resulting dye sensitized films were then thoroughly rinsed with ethanol, dried in an air stream, and stored in the dark. Details of the sample preparation and characterization of photon-induced sample damage are provided in the SI (S1, S3).

Time-Resolved XPS Experiment. The experiment was performed at the Soft X-ray Materials Science (SXR) instrument of the Linac Coherent Light Source (LCLS). An ultrashort (fwhm ≤50 fs) laser pulse with a center wavelength of 535 nm electronically excited the ruthenium dye complex. The transient electronic structure was probed by a time-delayed X-ray pulse (fwhm ≤100 fs) centered at 850 eV using a monochromator. Femtosecond time-resolved inner shell photoelectron spectra were recorded with a hemispherical electron analyzer (Scienta R3000). The uncertainty in the pump−probe time-delay Δt was ∼280 fs (fwhm). The pump laser was operated at 60 Hz, which is half the repetition rate of the LCLS (120 Hz), enabling the simultaneous recording of pump-on and pump-off spectra, which strongly suppresses the impact of experimental drifts on the pump-on/pump-off difference spectra. A detailed description of the experiment and data analysis is given in the SI (S2−S4).

Theoretical Modeling by Constrained Density Functional Theory. Structural optimizations were performed using plane-wave pseudopotential-based DFT[33,34] as implemented in the VASP[43] package. A plane-wave cutoff of 350 eV and pseudopotentials with the following valence electronic configurations were employed: $Zn(3d^{10}4s^2)$, $O(2s^22p^4)$, $C(2s^22p^2)$, $N(2s^22p^3)$, $S(3s^23p^4)$, $H(1s^1)$, $Ru(5s^14d^7)$. Exchange-correlation effects were modeled using the Perdew−Burke−Ernzerhoff[44] form of the generalized gradient approximation. The Brillouin zone was sampled at the Γ point. Structures were optimized until all forces were <0.04 eV/Å. Excited-state energies and associated core-level shifts (ΔE_b) were calculated through CDFT,[37] as implemented in the NWChem code,[45] using three different DFT functionals: BLYP,[38,39] B3LYP,[40,41] and CAM-B3LYP.[42] Ru was modeled using the Sapporo-DZP-2012[46] all-electron basis set, while N, C, S, Zn, and O were modeled using the SBKJC[47,48] basis set and associated effective core potential (ECP). H was described through the 6-311+G* basis set. Ru 3d core-level shifts were estimated using the initial state rule as differences in core-level eigenvalues of ground and valence excited states. Further details are provided in the SI (S5).

dx.doi.org/10.1021/jz501264x | J. Phys. Chem. Lett. 2014, 5, 2753−2759

■ ASSOCIATED CONTENT

Supporting Information

S1. Sample preparation, S2. Time-resolved XPS experiment, S3. Sample damage measurements and control, S4. Data analysis, S5. Theoretical modeling by constrained density functional theory (CDFT). This material is available free of charge via the Internet at http://pubs.acs.org.

■ AUTHOR INFORMATION

Corresponding Author

*E-mail: ogessner@lbl.gov.

Present Addresses

□KR.S.: Leibniz Institute of Surface Modification, 04138 Leipzig, Germany.

●A.A.C.: Chemical Sciences Division, Lawrence Berkeley National Laboratory, Berkeley, CA 94720, USA.

△J.V.-W. and M.-F.L.: Department of Chemistry, University of Illinois at Urbana−Champaign, Urbana, IL 61801, USA.

▲F.W.: Berliner Glas KGaA, 12347 Berlin, Germany.

▼M.L.S.: SLAC National Accelerator Laboratory, Menlo Park, CA 94025, USA.

%C.K.: Centre for Quantum Dynamics, Griffith University, Nathan, Qld 4111, Australia.

&M.M.: National Science Foundation BioXFEL Science and Technology Center, Buffalo, NY 14203, USA.

Notes

The authors declare no competing financial interest.

■ ACKNOWLEDGMENTS

This work was supported by the U.S. Department of Energy, Office of Basic Energy Sciences, Chemical Sciences, Geosciences and Biosciences Division, through contract no. DE-AC02-05CH11231. O.G. was supported by the Department of Energy Office of Science Early Career Research Program. K.R.S. was supported by the Alexander von Humboldt foundation. S.R.L. and J.V.-W. were supported by the NSSEFF program of the Department of Defense. Ab initio modeling by C.D.P. and D.P. was performed as part of a user project at The Molecular Foundry, Lawrence Berkeley National Laboratory (LBNL) and using high-performance computing resources of The Molecular Foundry and of the National Energy Research Scientific Computing Center (NERSC) at LBNL. J.Z.Z. is grateful for support by the Basic Energy Sciences Division of the U.S. DOE (DE-FG02-ER46232). Portions of this research were carried out on the SXR Instrument at the Linac Coherent Light Source (LCLS), a division of SLAC National Accelerator Laboratory and an Office of Science user facility operated by Stanford University for the U.S. Department of Energy. The SXR Instrument is funded by a consortium whose membership includes the LCLS, Stanford University through the Stanford Institute for Materials Energy Sciences (SIMES), LBNL, University of Hamburg through the BMBF priority program FSP 301, and the Center for Free Electron Laser Science (CFEL). We appreciate the support received from T. Tyliszczak, M. P. Hertlein, P. A. Heimann, A. R. Nilsson, and M. Beye as well as the staff at LCLS and the Advanced Light Source (ALS) at LBNL.

■ REFERENCES

(1) O'Regan, B.; Grätzel, M. A Low-Cost, High-Efficiency Solar-Cell Based on Dye-Sensitized Colloidal TiO_2 Films. *Nature* **1991**, *353*, 737−740.

(2) Hagfeldt, A.; Boschloo, G.; Sun, L. C.; Kloo, L.; Pettersson, H. Dye-Sensitized Solar Cells. *Chem. Rev.* **2010**, *110*, 6595−6663.

(3) Peter, L. M. The Grätzel Cell: Where Next? *J. Phys. Chem. Lett.* **2011**, *2*, 1861−1867.

(4) Jung, H. S.; Lee, J.-K. Dye Sensitized Solar Cells for Economically Viable Photovoltaic Systems. *J. Phys. Chem. Lett.* **2013**, *4*, 1682−1693.

(5) Anderson, N. A.; Lian, T. Q. Ultrafast Electron Transfer at the Molecule-Semiconductor Nanoparticle Interface. *Annu. Rev. Phys. Chem.* **2005**, *56*, 491−519.

(6) Benkö, G.; Kallioinen, J.; Myllyperkiö, P.; Trif, F.; Korppi-Tommola, J. E. I.; Yartsev, A. P.; Sundström, V. Interligand Electron Transfer Determines Triplet Excited State Electron Injection in RuN3-Sensitized TiO_2 films. *J. Phys. Chem. B* **2004**, *108*, 2862−2867.

(7) Kallioinen, J.; Benkö, G.; Sundström, V.; Korppi-Tommola, J. E. I.; Yartsev, A. P. Electron Transfer from the Singlet and Triplet Excited States of $Ru(dcbpy)_2(NCS)_2$ into Nanocrystalline TiO_2 Thin Films. *J. Phys. Chem. B* **2002**, *106*, 4396−4404.

(8) Furube, A.; Katoh, R.; Hara, K.; Murata, S.; Arakawa, H.; Tachiya, M. Ultrafast Stepwise Electron Injection from Photoexcited Ru-Complex into Nanocrystalline ZnO Film via Intermediates at the Surface. *J. Phys. Chem. B* **2003**, *107*, 4162−4166.

(9) Katoh, R.; Furube, A.; Yoshihara, T.; Hara, K.; Fujihashi, G.; Takano, S.; Murata, S.; Arakawa, H.; Tachiya, M. Efficiencies of Electron Injection from Excited N3 Dye into Nanocrystalline Semiconductor (ZrO_2, TiO_2, ZnO, Nb_2O_5, SnO_2, In_2O_3) Films. *J. Phys. Chem. B* **2004**, *108*, 4818−4822.

(10) Němec, H.; Rochford, J.; Taratula, O.; Galoppini, E.; Kužel, P.; Polívka, T.; Yartsev, A.; Sundström, V. Influence of the Electron-Cation Interaction on Electron Mobility in Dye-Sensitized ZnO and TiO_2 Nanocrystals: A Study Using Ultrafast Terahertz Spectroscopy. *Phys. Rev. Lett.* **2010**, *104*, 197401.

(11) Strothkämper, C.; Bartelt, A.; Sippel, P.; Hannappel, T.; Schütz, R.; Eichberger, R. Delayed Electron Transfer through Interface States in Hybrid ZnO/Organic-Dye Nanostructures. *J. Phys. Chem. C* **2013**, *117*, 17901−17908.

(12) Stockwell, D.; Yang, Y.; Huang, J.; Anfuso, C.; Huang, Z. Q.; Lian, T. Q. Comparison of Electron-Transfer Dynamics from Coumarin 343 to TiO_2, SnO_2, and ZnO Nanocrystalline Thin Films: Role of Interface-Bound Charge-Separated Pairs. *J. Phys. Chem. C* **2010**, *114*, 6560−6566.

(13) Tiwana, P.; Docampo, P.; Johnston, M. B.; Snaith, H. J.; Herz, L. M. Electron Mobility and Injection Dynamics in Mesoporous ZnO, SnO_2, and TiO_2 Films Used in Dye-Sensitized Solar Cells. *ACS Nano* **2011**, *5*, 5158−5166.

(14) Bräm, O.; Cannizzo, A.; Chergui, M. Ultrafast Fluorescence Studies of Dye Sensitized Solar Cells. *Phys. Chem. Chem. Phys.* **2012**, *14*, 7934−7937.

(15) Britton, A. J.; Weston, M.; O'Shea, J. N. Charge Transfer from an Aromatic Adsorbate to a Semiconductor TiO_2 Surface Probed on the Femtosecond Time Scale with Resonant Inelastic X-Ray Scattering. *Phys. Rev. Lett.* **2012**, *109*, 017401.

(16) Schnadt, J.; Brühwiler, P. A.; Patthey, L.; O'Shea, J. N.; Södergren, S.; Odelius, M.; Ahuja, R.; Karis, O.; Bässler, M.; Persson, P.; et al. Experimental Evidence for Sub-3-fs Charge Transfer from an Aromatic Adsorbate to a Semiconductor. *Nature* **2002**, *418*, 620−623.

(17) Rehm, J. M.; McLendon, G. L.; Nagasawa, Y.; Yoshihara, K.; Moser, J.; Grätzel, M. Femtosecond Electron-Transfer Dynamics at a Sensitizing Dye-Semiconductor (TiO_2) Interface. *J. Phys. Chem.* **1996**, *100*, 9577−9578.

(18) Van Kuiken, B. E.; Huse, N.; Cho, H.; Strader, M. L.; Lynch, M. S.; Schoenlein, R. W.; Khalil, M. Probing the Electronic Structure of a Photoexcited Solar Cell Dye with Transient X-ray Absorption Spectroscopy. *J. Phys. Chem. Lett.* **2012**, *3*, 1695−1700.

(19) Zhang, X. Y.; Smolentsev, G.; Guo, J. C.; Attenkofer, K.; Kurtz, C.; Jennings, G.; Lockard, J. V.; Stickrath, A. B.; Chen, L. X. Visualizing Interfacial Charge Transfer in Ru-Dye-Sensitized TiO_2 Nanoparticles Using X-ray Transient Absorption Spectroscopy. *J. Phys. Chem. Lett.* **2011**, *2*, 628−632.

(20) Lemke, H. T.; Bressler, C.; Chen, L. X.; Fritz, D. M.; Gaffney, K. J.; Galler, A.; Gawelda, W.; Haldrup, K.; Hartsock, R. W.; Ihee, H.; et al.

Femtosecond X-ray Absorption Spectroscopy at a Hard X-ray Free Electron Laser: Application to Spin Crossover Dynamics. *J. Phys. Chem. A* **2013**, *117*, 735−740.
(21) Huang, J.; Buyukcakir, O.; Mara, M. W.; Coskun, A.; Dimitrijevic, N. M.; Barin, G.; Kokhan, O.; Stickrath, A. B.; Ruppert, R.; Tiede, D. M.; et al. Highly Efficient Ultrafast Electron Injection from the Singlet MLCT Excited State of Copper(I) Diimine Complexes to TiO_2 Nanoparticles. *Angew. Chem., Int. Ed.* **2012**, *51*, 12711−12715.
(22) Rittmann-Frank, M. H.; Milne, C. J.; Rittmann, J.; Reinhard, M.; Penford, T. J.; Chergui, M. Mapping of the Photoinduced Electron Traps in TiO_2 by Picosecond X-ray Absorption Spectroscopy. *Angew. Chem., Int. Ed.* **2014**, *53*, 5858−5862.
(23) Monat, J. E.; Rodriguez, J. H.; McCusker, J. K. Ground- and Excited-State Electronic Structures of the Solar Cell Sensitizer bis(4,4′-dicarboxylato-2,2′-bipyridine)bis(isothiocyanato)ruthenium(II). *J. Phys. Chem. A* **2002**, *106*, 7399−7406.
(24) De Angelis, F.; Fantacci, S.; Selloni, A.; Nazeeruddin, M. K.; Grätzel, M. First-Principles Modeling of the Adsorption Geometry and Electronic Structure of Ru(II) Dyes on Extended TiO_2 Substrates for Dye-Sensitized Solar Cell Applications. *J. Phys. Chem. C* **2010**, *114*, 6054−6061.
(25) Jiao, Y.; Ding, Z. J.; Meng, S. Atomistic Mechanism of Charge Separation upon Photoexcitation at the Dye-Semiconductor Interface for Photovoltaic Applications. *Phys. Chem. Chem. Phys.* **2011**, *13*, 13196−13201.
(26) Le Bahers, T.; Pauporté, T.; Lainé, P. P.; Labat, F.; Adamo, C.; Ciofini, I. Modeling Dye-Sensitized Solar Cells: From Theory to Experiment. *J. Phys. Chem. Lett.* **2013**, *4*, 1044−1050.
(27) Pietzsch, A.; Föhlisch, A.; Beye, M.; Deppe, M.; Hennies, F.; Nagasono, M.; Suljoti, E.; Wurth, W.; Gahl, C.; Döbrich, K.; et al. Towards Time Resolved Core Level Photoelectron Spectroscopy with Femtosecond X-Ray Free-Electron Lasers. *New J. Phys.* **2008**, *10*, 033004.
(28) Marsi, M.; Couprie, M. E.; Nahon, L.; Garzella, D.; Hara, T.; Bakker, R.; Billardon, M.; Delboulbé, A.; Indlekofer, G.; Taleb-Ibrahimi, A. Surface States and Space Charge Layer Dynamics on Si(111)2 × 1: A Free Electron Laser-Synchrotron Radiation Study. *Appl. Phys. Lett.* **1997**, *70*, 895−897.
(29) Bersch, E. *Energy Level Alignment In Metal/Oxide/Semiconductor and Organic Dye/Oxide Systems*. Ph.D. Thesis, Ruttgers University, 2008.
(30) Quintana, M.; Edvinsson, T.; Hagfeldt, A.; Boschloo, G. Comparison of Dye-Sensitized ZnO and TiO_2 Solar Cells: Studies of Charge Transport and Carrier Lifetime. *J. Phys. Chem. C* **2007**, *111*, 1035−1041.
(31) Anta, J. A.; Guillén, E.; Tena-Zaera, R. ZnO-Based Dye-Sensitized Solar Cells. *J. Phys. Chem. C* **2012**, *116*, 11413−11425.
(32) Mayor, L. C.; Ben Taylor, J.; Magnano, G.; Rienzo, A.; Satterley, C. J.; O'Shea, J. N.; Schnadt, J. Photoemission, Resonant Photoemission, and X-Ray Absorption of a Ru(II) Complex Adsorbed on Rutile TiO_2(110) Prepared by In Situ Electrospray Deposition. *J. Chem. Phys.* **2008**, *129*, 114701.
(33) Hohenberg, P.; Kohn, W. Inhomogeneous Electron Gas. *Phys. Rev. A* **1964**, *136*, B864−B871.
(34) Kohn, W.; Sham, L. J. Self-Consistent Equations Including Exchange and Correlation Effects. *Phys. Rev.* **1965**, *140*, 1133−1138.
(35) Keis, K.; Lindgren, J.; Lindquist, S. E.; Hagfeldt, A. Studies of the Adsorption Process of Ru Complexes in Nanoporous ZnO Electrodes. *Langmuir* **2000**, *16*, 4688−4694.
(36) Rensmo, H.; Södergren, S.; Patthey, L.; Westermark, K.; Vayssieres, L.; Kohle, O.; Brühwiler, P. A.; Hagfeldt, A.; Siegbahn, H. The Electronic Structure of the cis-bis(4,4′-dicarboxy-2,2′-bipyridine)-bis(isothiocyanato)ruthenium(II) Complex and its Ligand 2,2′-bipyridyl-4,4′-dicarboxylic Acid Studied with Electron Spectroscopy. *Chem. Phys. Lett.* **1997**, *274*, 51−57.
(37) Kaduk, B.; Kowalczyk, T.; Van Voorhis, T. Constrained Density Functional Theory. *Chem. Rev.* **2012**, *112*, 321−370.
(38) Becke, A. D. Density-Functional Exchange-Energy Approximation with Correct Asymptotic-Behavior. *Phys. Rev. A* **1988**, *38*, 3098−3100.
(39) Lee, C. T.; Yang, W. T.; Parr, R. G. Development of the Colle-Salvetti Correlation-Energy Formula into a Functional of the Electron-Density. *Phys. Rev. B* **1988**, *37*, 785−789.
(40) Stephens, P. J.; Devlin, F. J.; Chabalowski, C. F.; Frisch, M. J. Ab-Initio Calculation of Vibrational Absorption and Circular-Dichroism Spectra Using Density-Functional Force-Fields. *J. Phys. Chem.* **1994**, *98*, 11623−11627.
(41) Kim, K.; Jordan, K. D. Comparison of Density-Functional and MP2 Calculations on the Water Monomer and Dimer. *J. Phys. Chem.* **1994**, *98*, 10089−10094.
(42) Yanai, T.; Tew, D. P.; Handy, N. C. A New Hybrid Exchange-Correlation Functional Using the Coulomb-Attenuating Method (CAM-B3LYP). *Chem. Phys. Lett.* **2004**, *393*, 51−57.
(43) Kresse, G.; Furthmuller, J. Efficient Iterative Schemes for Ab Initio Total-Energy Calculations Using a Plane-Wave Basis Set. *Phys. Rev. B* **1996**, *54*, 11169−11186.
(44) Perdew, J. P.; Burke, K.; Ernzerhof, M. Generalized Gradient Approximation Made Simple. *Phys. Rev. Lett.* **1996**, *77*, 3865−3868.
(45) Valiev, M.; Bylaska, E. J.; Govind, N.; Kowalski, K.; Straatsma, T. P.; Van Dam, H. J. J.; Wang, D.; Nieplocha, J.; Apra, E.; Windus, T. L.; et al. NWChem: A Comprehensive and Scalable Open-Source Solution for Large Scale Molecular Simulations. *Comput. Phys. Commun.* **2010**, *181*, 1477−1489.
(46) Noro, T.; Sekiya, M.; Koga, T. Segmented Contracted Basis Sets for Atoms H Through Xe: Sapporo-(DK)-nZP Sets (n = D, T, Q). *Theor. Chem. Acc.* **2012**, *131*, 1124.
(47) Stevens, W. J.; Basch, H.; Krauss, M. Compact Effective Potentials and Efficient Shared-Exponent Basis-Sets for the 1st-Row and 2nd-Row Atoms. *J. Chem. Phys.* **1984**, *81*, 6026−6033.
(48) Stevens, W. J.; Krauss, M.; Basch, H.; Jasien, P. G. Relativistic Compact Effective Potentials and Efficient, Shared-Exponent Basis-Sets for the 3rd-Row, 4th-Row, and 5th-Row Atoms. *Can. J. Chem.* **1992**, *70*, 612−630.